Tectonic stress accumulation in Bohai–Zhangjiakou Seismotectonic Zone based on 3D visco-elastic modelling

Ju Wei[1,*], Sun Weifeng[1], Ma Xiaojing[2,3] and Jiang Hui[3]

[1]*School of Resources and Geoscience, China University of Mining and Technology, Xuzhou 221116, China.*
[2]*College of Resources, Shijiazhuang University of Economics, Shijiazhuang 050031, China.*
[3]*Institute of Geology and Geophysics, Chinese Academy of Sciences, Beijing 100029, China.*
[*]*Corresponding author. e-mail: wju@cumt.edu.cn*

Future earthquake potential in the Bohai–Zhangjiakou Seismotectonic Zone (BZSZ) in North China deserves close attention. Tectonic stress accumulation state is an important indicator for earthquakes; therefore, this study aims to analyse the stress accumulation state in the BZSZ via three-dimensional visco-elastic numerical modelling. The results reveal that the maximum shear stress in the BZSZ increases gradually as the depth increases, and the stress range is wider in the lower layer. In the upper layer, the maximum shear stress is high in the Zhangjiakou area, whereas in the lower layer, relatively high values occur in the Penglai–Yantai area, which may be affected by the depth of the Moho surface. Besides, weak fault zones will be easily fractured when the maximum shear stress is not sufficiently high due to their low strengths, resulting in earthquakes. Therefore, based on the modelling results, the upper layer of the Zhangjiakou area and the lower layer of the Penglai–Yantai area in the BZSZ in North China are more likely to experience earthquakes.

1. Introduction

The Bohai–Zhangjiakou Seismotectonic Zone (BZSZ) is situated in the northern part of the North China seismic region and is over 700 km long and 250 km wide in the NW–SE direction. The BZSZ, containing nearly 20 discontinuous NW–NWW-trending faults (Gao and Ma 1993; Xu *et al.* 1998; Fang and Zhang 2009; Suo *et al.* 2013; figure 1), is a left-lateral slip structure and has an important controlling effect on regional tectonics (Hou *et al.* 1999; Fu *et al.* 2004).

Several earthquakes have occurred in the BZSZ (Gao and Ma 1993; Fu *et al.* 2004; figure 1), including the 1679 Sanhe–Pinggu earthquake (Ms = 8.0; Xiang *et al.* 1988) and the 1976 Tangshan earthquake (Ms = 7.8; Chen *et al.* 1979; Liu *et al.* 2007) that have caused significant damage to life and property. During the past several decades, studies have been performed to analyse and explain the seismogenic mechanisms of these earthquakes. The Tangshan earthquake for example, occurred in the contiguous part between the Yanshan fold belt and the depression of North China Plain. The observational aftershock sequence of the Tangshan earthquake was distributed primarily in the Tangshan fault-block in the NE 45° direction (Xue 1986; Liu *et al.* 2007). Furthermore, previous studies on earthquake geology demonstrated that the Tangshan earthquake was formed under the action of constant forces along the boundaries of an inhomogeneous medium, which led to the accumulation of elastic energy in the local area (Song *et al.* 1982; Mei and Liang 1989). In addition, Feng *et al.*

Keywords. Bohai–Zhangjiakou Seismotectonic Zone; tectonic stress accumulation; visco-elastic modelling; Moho surface; modern tectonic stress field.

(1996) studied and analysed the seismogenic condition and long-term precursors of the Tangshan earthquake.

It is important to study how tectonic stress accumulates in the BZSZ in North China during long-term compressional processes and what the tectonic stress accumulation state is in the lithosphere. These issues require considerable attention and need to be addressed in terms of geomechanics and numerical modelling because the tectonic stress accumulation state is an important indicator for earthquakes. The present study aims to analyse the tectonic stress accumulation state in the BZSZ using three-dimensional (3D) visco-elastic modelling and discuss the effect of Moho surface on this stress accumulation.

2. Geological setting

The BZSZ in North China extends along Bohai Bay–Tianjin–Beijing–Zhangjiakou. Based on interpretations from satellite photographs, the BZSZ may include a NWW trending hidden active fault, which is approximately 180 km long from Beijing to North Tianjin (Xu *et al.* 1998; Li *et al.* 1999). Recently, an increasing number of studies have focused on the deep structures of the BZSZ, where both Cenozoic tectonic activity and seismicity have been extremely intensive and frequent (Zhang *et al.* 2002; Wang *et al.* 2004).

In general, the BZSZ is a left-lateral slip and has an important controlling effect on regional tectonics in North China (Hou *et al.* 1999; Fu *et al.* 2004; Wang *et al.* 2005; Fang and Zhang 2009). Seismic reflection profiles across the BZSZ have shown the presence of several deeply buried faults cutting the lithosphere (Gao 2001; Lai *et al.* 2006). During the past several decades, continuous Global Positioning System (GPS) observations have revealed relative sinistral movement between the Yanshan Mountains and the North China Basin (Yang *et al.* 2002; Wang *et al.* 2005). In addition, some anomalous geophysical backgrounds of the lithosphere exist in the BZSZ. According to an investigation of magnetotelluric data, the BZSZ is also a low resistivity zone in the lithosphere under North China (Zhao *et al.* 1997).

Records indicate that seven historical and recent earthquakes with Ms $\geq$ 7.0 have occurred in the BZSZ (Fu *et al.* 2004; table 1), and the majority of these strong seismic activities have occurred at intersections between the NW-trending BZSZ and the NE-trending seismotectonic zones, such as the Tanchen Lujiang Seismotectonic Zone (Wang *et al.* 2005; figure 1). Based on studies of the field geology, crustal deformation, geophysical field, topography, seismic parameters and the relationship between NE- and NW-trending faults, the NW-trending BZSZ can be divided into four segments with various seismic characteristics and episodes, namely, the Penglai–Yantai, Tangshan–Bohai, Beijing and Zhangjiakou segments (figure 2; Gao *et al.* 2001).

Both paleo and modern tectonic stresses are fundamental datasets in Earth sciences (Zoback 1992; Sperner *et al.* 2003; Delvaux and Barth 2010; Ju *et al.* 2013a), and investigations into crustal tectonic stress are extremely important in Earth geotectonic studies (Lunina and Gladkov 2007; Ju *et al.* 2013a, b). In general, several types of data, including earthquake focal mechanisms, can allow and facilitate a revisiting of tectonic interpretations of the modern crustal stress field (Zoback 1992; Angelier 2002; Delvaux and Sperner 2003; Delvaux and Barth 2010). The average direction of the modern maximum principal stress axis in the BZSZ in North China is interpreted to be consistently NEE–SWW (figure 3).

3. 3D visco-elastic modelling

In this study, a 3D visco-elastic model was run using the Finite Element (FE) technique to study the stress accumulation state in the BZSZ in North China. FE modelling allows complex geometries (e.g., mechanical layers and faults) to be combined

Table 1. *Catalog of strong earthquakes (Ms $\geq$ 7.0) in the BZSZ in North China since 1000–2000 AD (after Fu et al. 2004).*

Date	Latitude (°N)	Longitude (°E)	Ms	Location
1548-09-12	38.0	121.0	7.0	Bohai Bay
1597-10-06	38.5	120.0	7.0	Bohai Bay
1626-06-28	39.4	114.2	7.0	Lingqiu, Shanxi
1679-09-02	40.0	117.0	8.0	Sanhe-Pinggu, Beijing
1888-06-13	38.5	119.2	7.5	Bohai Bay
1969-07-18	38.3	119.4	7.4	Bohai Bay
1976-07-28	39.4	118.0	7.8	Tangshan, Hebei

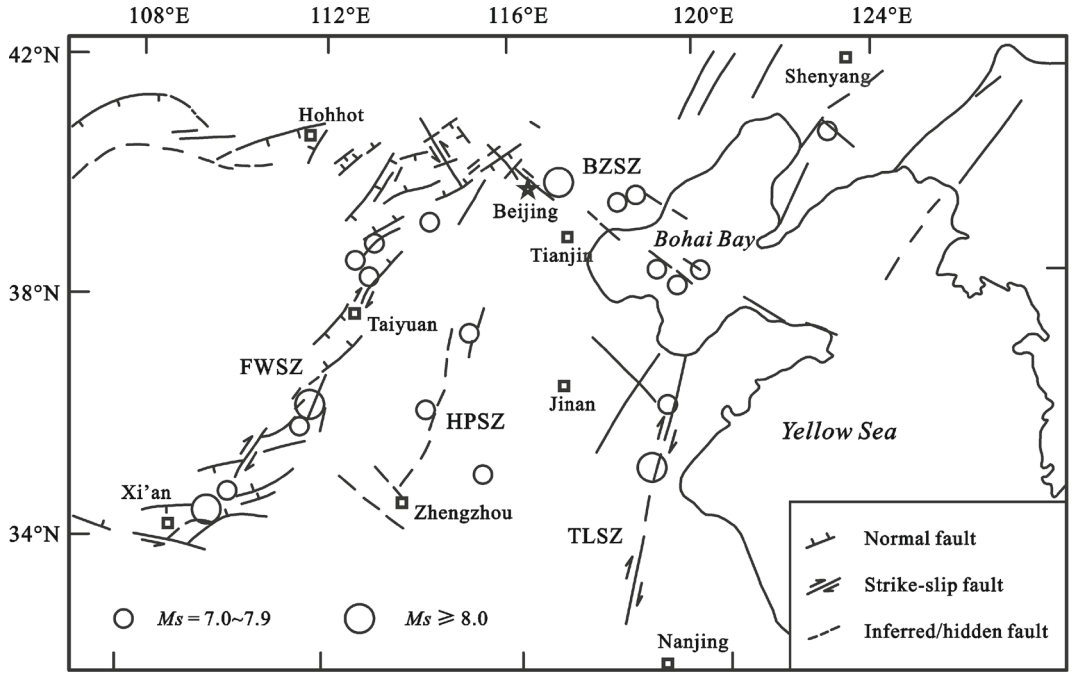

Figure 1. Seismotectonic sketch map in North China (after Xu *et al.* 1998). BZSZ: Bohai–Zhangjiakou Seismotectonic Zone, TLSZ: Tancheng–Lujiang Seismotectonic Zone, HPSZ: Hebei Plain Seismotectonic Zone, and FWSZ: Fenwei Seismotectonic Zone.

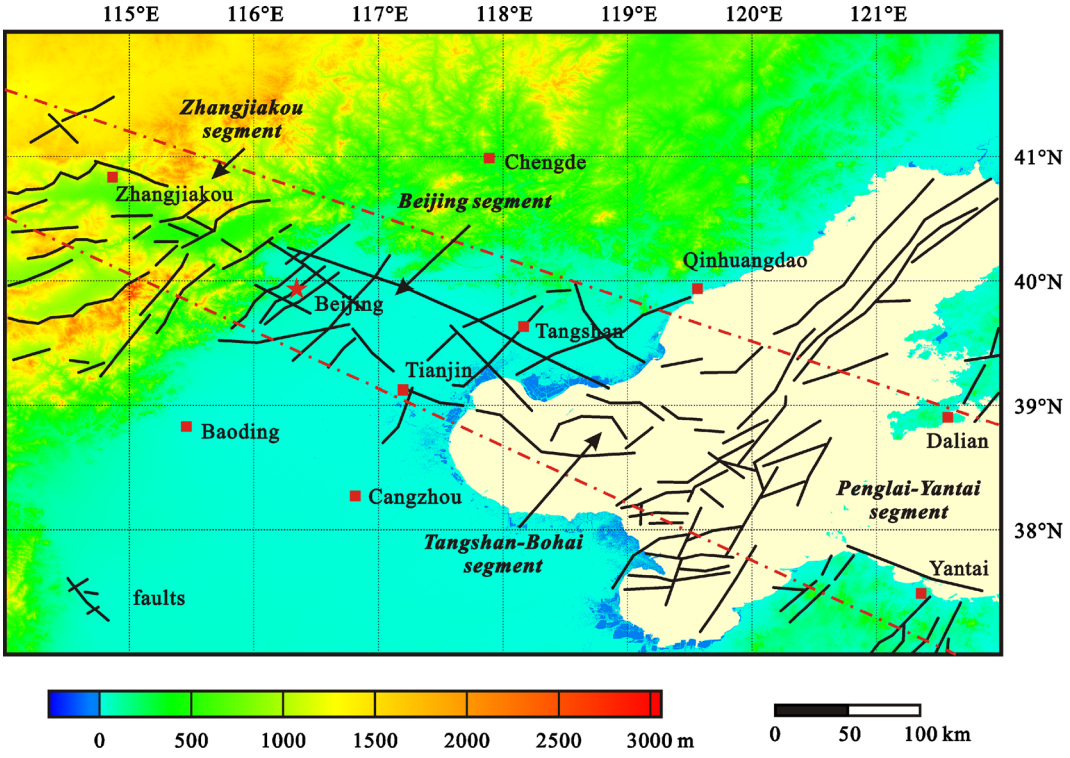

Figure 2. Fault distribution and tectonic segmentation in the BZSZ in North China. The BZSZ is divided into four segments: the Penglai–Yantai segment, Tangshan–Bohai segment, Zhangjiakou segment and Beijing segment. The faults data are from Gao *et al.* (2001) and Han (2009).

with realistic material parameters to produce physically realistic and mechanically rigorous models (Yin 1991; Smart *et al.* 2009; Ju *et al.* 2013b, 2014). The general-purpose FE code ANSYS was used in this study because it is well suited to analyse these type of problems over a wide range of scales in

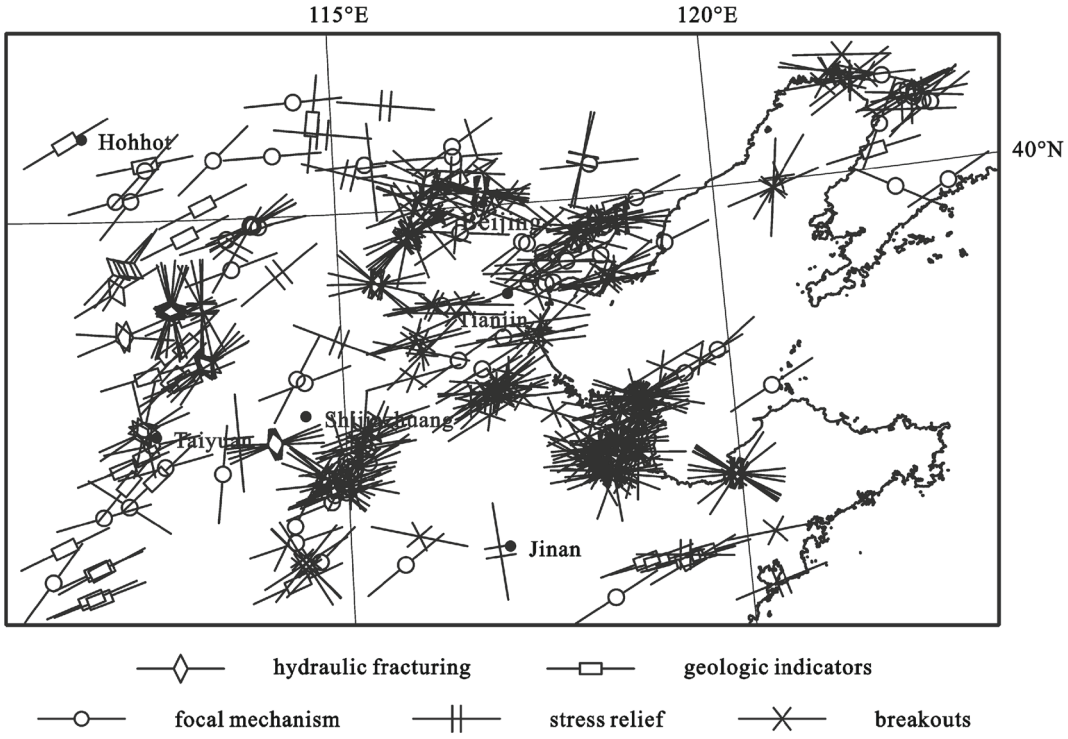

Figure 3. Modern tectonic stress field in North China (stress indicator data are from China Earthquake Networks Center).

one, two and three dimensions (Hou *et al.* 2010; Jarosinski *et al.* 2011; Ju *et al.* 2013a, b).

3.1 *Geometry*

In the present study, complex model geometries were constructed based on the CRUST 1.0 data (Laske *et al.* 2013; figure 4). A larger rectangular area including the BZSZ was selected to construct the model and to avoid the boundary effects. The x-, y- and z-axes indicate the east, north and vertical (depth) directions, and the depth ranges from the surface to 80 km underground. In the vertical direction, the 80 km depth was divided into four layers: the upper crust, middle crust, lower crust and upper mantle (figure 4).

Multiple faults have developed in the Zhangjiakou–Bohai area in North China, and several important ones were selected to be included in the model because they were active in the Late Pleistocene and Holocene periods, and earthquakes had occurred at least once on these faults (table 2 and figure 4). In general, faults can be considered in two ways during FE modelling. The first approach implements the existing faults as discrete planes of weakness cutting the FE model. These planes are described by so-called contact elements, which are defined at opposite sides of pre-assigned faults (Smart *et al.* 2009; Fischer and Henk 2013; Ju *et al.* 2014). In the second approach, which was used in the present study, the entire FE model

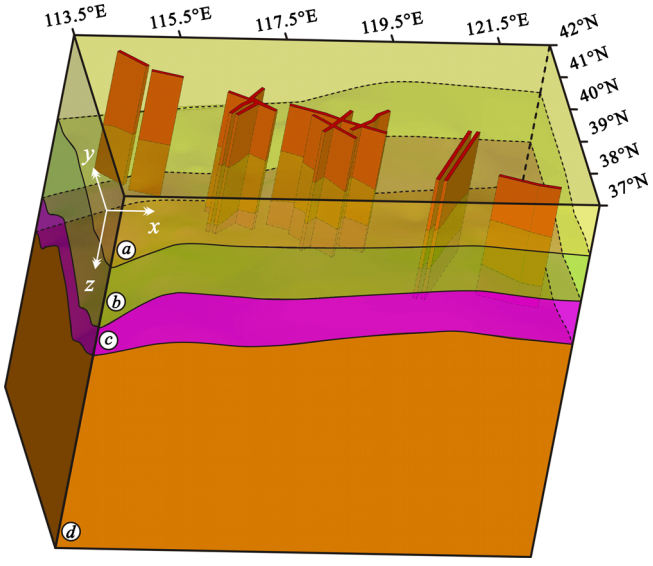

Figure 4. Three-dimensional finite element model in the Bohai–Zhangjiakou area. x: the east direction; y: the north direction; z: the vertical (depth) direction. For clarity, this showing model utilized a ratio of $x : y : z = 1 : 1 : 10$. (**a**) Upper crust layer, (b) middle crust layer, (c) lower crust layer, and (d) upper mantle layer.

meshes continuously and the faults are represented by weakness zones (Fischer and Henk 2013; Ju *et al.* 2013a, b).

All the four layers and faults in the model were discretized using primarily three-node triangular elements with some four-node quadrilateral elements, and after meshing, there were approximately 28543 nodes and 158839 elements (figure 5).

Table 2. *The important faults developed in the Bohai–Zhangjiakou area and their parameters (the data are after Gao and Ma 1993; Chen et al. 1999; Li et al. 1999; Gao 2001; Xu et al. 2002; Wang and Li 2005; Li et al. 2009; Hu 2010; Zhan et al. 2011).*

Faults	Length	Strike	Dip	Dip angle	Lastest activity	Fault pattern
Miaodongying–Dayingtan Fault*	35 km	NW–SE			Q_4(?)	
Zhangjiakou Fault*	30 km	NW–SE	SW	60	Q_3	Normal
Xianmalin Fault	15 km	NW–SE	SW	75–80	Q_4	Normal
Shizhuang Fault	20 km	NW–SE	NE	70–80	Q_2	Normal-strike slip
Xinbaoan–Shacheng Fault	32 km	NW–SE	SW	60–70	Q_4	Normal
Huangtuyao–Tumu Fault	21 km	NW–SE	SW	60	Q_3	Normal
Sanggan River Fault	32 km	E–W	N	70	Q_3	Normal
South Yihua Basin Fault	16 km	E–W	N	55–65	Q_4	
Nankou–Sunhe Fault*	58 km	NW–SE	SW/NE	70	Q_4	Normal
Yongding River Fault	26 km	NW–SE	SW/NE	70–75	Q_2	Normal-strike slip
Changping–Fengnan Fault*	180 km	NW–SE	SW	50–70	Q_2	Normal-strike slip
Huangzhuang–Gaoliying Fault*	130 km	NE–SW	SE	55–75	Q_3	Normal
Shunyi–Liangxiang Fault	110 km	NNE–SSW	NW	60–80	Q_3	Normal
Xiadian Fault*	100 km	NE–SW	SE	70–80	Q_4	Normal
Langfang–Wuqing Fault	50 km	NW–SE	SW		Q_3	Normal
Nanyuan–Tongxian Fault		NE–SW	NW		Q_1(?)	Normal
Nankou Piedmont Fault	60 km	NE–SW	SE	50–80	Q_3	Normal
Luanxian–Leting Fault	50 km	NNW–SSE	NE	70–90(?)	Q_4(?)	Reverse
Jiyunhe Fault*	50 km	NW–SE	SW	70	Q_4	Normal
Tangshan Fault*	50 km	NE–SW	NW	70–80		Strike slip
Haihe Fault	70 km	NWW–SEE	SSW	60	Q	Normal
Baigezhuang Fault	50 km	NW–SE	SW	60	Q_{1-2}	Normal
Ninghe–Changli Fault*	160 km	NE–SW	SE	~85	Q_4	Normal
Bozhong No.2 Fault	34 km	NW–SE	NE		Q_4	Normal
Shaxi Fault		NW–SE	SSW	~90	Q_4	Normal
Chengbei Fault		NW–SE	SSW	~90	Q_3	Normal
Shanan Fault		NWW–SEE	SSW	~90	Q_3	Normal
Penglai–Weihai Fault*	140 km	NW–SE	NE		Q_{3-4}	Normal
Tancheng–Lujiang Fault Belt*		NNE–SSW	E	60		Strike slip

Note: Faults with stars are included in the finite element model. Q: Quaternary period; Q_1: Early Pleistocene epoch; Q_2: Middle Pleistocene epoch; Q_3: Late Pleistocene epoch; Q_4: Holocene epoch.

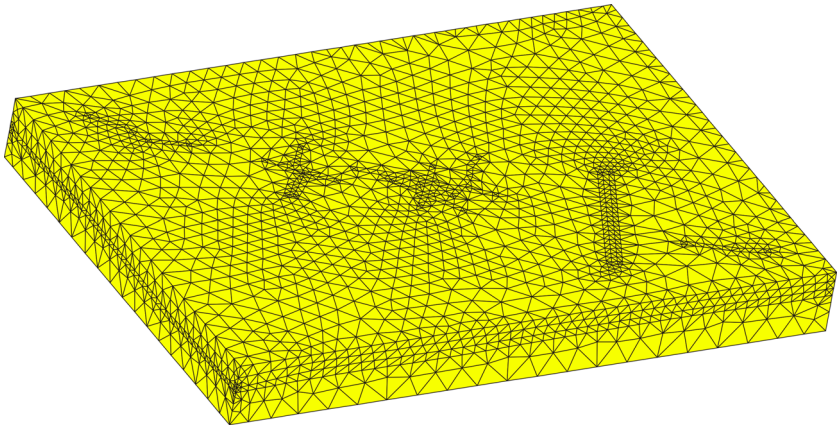

Figure 5. Meshing graph of the finite element model in the Bohai–Zhangjiakou area. There are altogether 28,543 nodes and 158,839 elements in the model.

3.2 *Material properties*

In the present study, material properties were assigned to the elements representing different layers and faults. Mechanical behaviour in the elastic domain was described by Hooke's law, whereas the viscous deformations obeyed Newton's law of viscosity (Jaeger *et al.* 2007).

Young's modulus and Poisson's ratio are the most important elastic parameters in building materials (Martinez-Martinez *et al.* 2012; Ju *et al.* 2014, 2015), and can be calculated from the wave velocity and density data (Liu *et al.* 1986; Rao *et al.* 2006).

$$E = \frac{\rho V_S^2 (3V_P^2 - 4V_S^2)}{V_P^2 - V_S^2} \quad (1)$$

$$\upsilon = \frac{V_p^2 - 2V_S^2}{2(V_p^2 - V_S^2)} \quad (2)$$

where E is the dynamic Young's modulus, υ is the Poisson's ratio, ρ is the density, V_P is the P-wave velocity, and V_S is the S-wave velocity.

Previous studies indicated that the ratio between the dynamic and static Young's moduli ranged from 0.8 to 3.0 (Mockovciakova and Pandula 2003; Martinez-Martinez *et al.* 2012; Yao *et al.* 2012) and that the dynamic Young's modulus was usually larger (Yao *et al.* 2012). Unfortunately, this ratio has not been quantitatively calculated in the study area; therefore, based on the geological settings of the BZSZ in North China, a ratio of 2.9 was used to calculate the static Young's modulus. The viscosities of the different layers in the visco-elastic FE model were based on the previous study results of Zang *et al.* (2003) and Shi and Cao (2008) (table 3).

Because the fault zones were defined as 'weak zones' in the FE model, the elastic modulus was typically smaller, and the Poisson's ratio was larger than that of a corresponding normal layer (Zeng *et al.* 2013). Therefore, in this study, the Young's modulus and Poisson's ratio were 50% and 105% of the corresponding normal layer, respectively (table 3).

3.3 *Boundary conditions*

According to the modern tectonic stress field shown in figure 3, the direction of the maximum principal stress axis is NEE–SWW in the study area. In addition, Li *et al.* (2006) calculated the current strain field with GPS data, and the average strain rate is approximately 0.5×10^{-9}/yr in the North China area. Based on previous studies (Xie *et al.* 2004; Wang *et al.* 2005; Li *et al.* 2006; Liu *et al.* 2012), the boundary conditions in this FE model were set as follows: (a) an average compressional displacement of 3.0 mm/yr was applied in the maximum principal stress axis NEE–SWW direction (Liu *et al.* 2012) with the horizontal displacement fixed on the west and south sides of the model, (b) the top of the model was set as a free boundary and the vertical displacement of the bottom was fixed to avoid movement and rotation of the model, and (c) a gravity load was applied to the entire model domain.

3.4 *Modelling results*

In the present study, the entire modelling process was performed in two steps. First, a gravity load was applied to the entire model domain. Once equilibrium was achieved, displacement boundary conditions were imposed to obtain the tectonic stress field. In the second step, each time step was set to 3 years, and the entire modelling process underwent 5000 steps.

The maximum shear stress accumulation was calculated and is shown at different depths in figure 6. In general, the maximum shear stress gradually increases with increasing depth, and a wider stress range exists in the lower layer (9 MPa at a depth of 25,000 m and 3.6 MPa at a depth of 5000 m; figure 6). In the lower layer, the maximum shear stress is higher in the Penglai–Yantai area, whereas in the upper layer, relatively high values are seen in the Zhangjiakou area (figure 6).

The maximum shear stress is low in the fault zones in all layers (figure 6) because these fault zones were set as 'weak zones' in the FE model. They have relatively low strengths and cannot accumulate stresses; therefore, these weak fault zones will be easily fractured, resulting in earthquakes. Based on the modelling results, the upper layer of the Zhangjiakou area and the lower layer of the Penglai–Yantai area in the BZSZ in North China are more likely to experience earthquakes.

Table 3. *Material properties used in the visco-elastic finite element model.*

Layers	h	ρ		E ($\times10^4$)		ν		η
		Normal layer	Faults	Normal layer	Faults	Normal layer	Faults	
Upper crust	−12.36	2750	2500	2.925	1.463	0.245	0.257	1.3×10^{23}
Middle crust	−24.53	2810	2600	3.452	1.726	0.252	0.265	2.0×10^{22}
Lower crust	−34.01	2930	2700	5.063	2.532	0.277	0.291	3.0×10^{20}
Upper mantle	–	3360	–	7.686	–	0.298	–	2.0×10^{21}

Note: h is the average depth (km), ρ is the density (kg/m^3), E is the static Young's modulus (MPa), ν is the Poisson's ratio, and η is the viscosity (Pa·s).

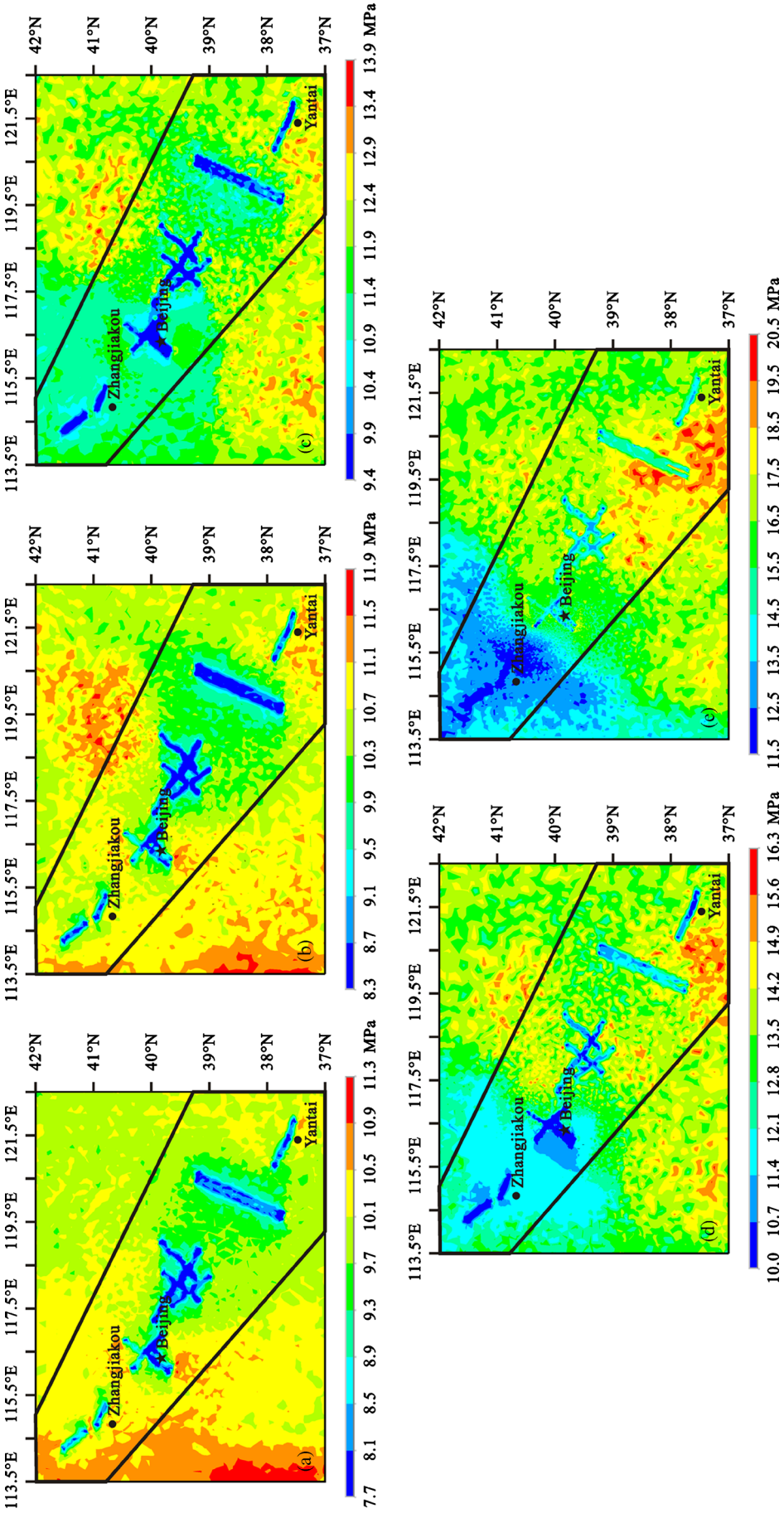

Figure 6. The maximum shear stress accumulation after 15,000 years in the BZSZ in North China. (a) –5000 m, (b) –10000 m, (c) –15000 m, (d) –20000 m, and (e) –25000 m.

4. Discussion and conclusions

During the Paleogene, multiple extensional structures consisting of numerous NNE-trending faults and graben systems were developed. There are several NWW-trending faults perpendicular to these systems that adjust the extension rate of different sections, with the Bohai–Zhangjiakou fault zone being the largest strike-slip transform zone in the area. In the Neogene and Quaternary periods, the tectonic movements in North China changed dramatically, and the Bohai–Zhangjiakou fault zone became a huge regional structure controlling the northern margin of the North China Basin (Xu *et al.* 1998; Wang *et al.* 2005).

In general, the movements of plates from the external boundary conditions are the primary causes of tectonic activities in the Chinese mainland (Chen *et al.* 2001). However, Yuan *et al.* (1999) proposed that the upward force produced by mantle convection might be the main driving force for earthquakes in North China, which experienced strong events during the Mesozoic period (Wu *et al.* 2005; Zhu *et al.* 2011, 2012). Therefore, earthquakes in the BZSZ are influenced by many factors, such as horizontal plate tectonics and fluctuations in the Moho surface.

The Moho surface is an extremely important factor for the tectonic stress accumulation state in the BZSZ (Xue 1986; Liu *et al.* 2012). The Moho surface is deeper in the Zhangjiakou area (figure 7), and the modelling results indicate that the maximum shear stress is high in the upper layer of this region, whereas, in the lower layer, the shear stress is relatively low (figure 6). This reveals that the depth of the Moho surface affects the tectonic stress accumulation state. In addition, Gao *et al.* (2001) proposed that both the NE- and NWW-trending faults were seismogenic tectonics in North China; however, the NE-trending faults were earthquake-generating tectonics, such as the Tangshan and Xiadian Faults (Xue 1986; Xiang *et al.* 1988; Liu *et al.* 2007; Suo *et al.* 2013). However, based on an analysis of the prospecting trenches, the NE-trending faults may not be seismogenic. The seismogenic process and modern seismic activity in North China are primarily controlled by NWW-trending faults (Suo *et al.* 2013). Seismogenic tectonics control stress accumulations and changes in the lithosphere, and usually are the major faults in the system, while earthquake-generating tectonics are channel to release tectonic stresses (Li and Wang 1981). In the BZSZ, seismogenic tectonics and earthquake-generating tectonics are not the same, similar to the Mabian–Yongshan Seismic Zone (Li and Wang 1981).

In the present study, the maximum shear stress accumulation in the BZSZ was calculated and shown at different depths based on 3D visco-elastic modelling. The maximum shear stress in the BZSZ increases gradually with increasing depth, and there is a wider stress range in the lower layer. In the upper layer, the calculated maximum shear stress is high in the Zhangjiakou area, whereas in the lower layer, the values are relatively high in the Penglai–Yantai area, which may be affected by the

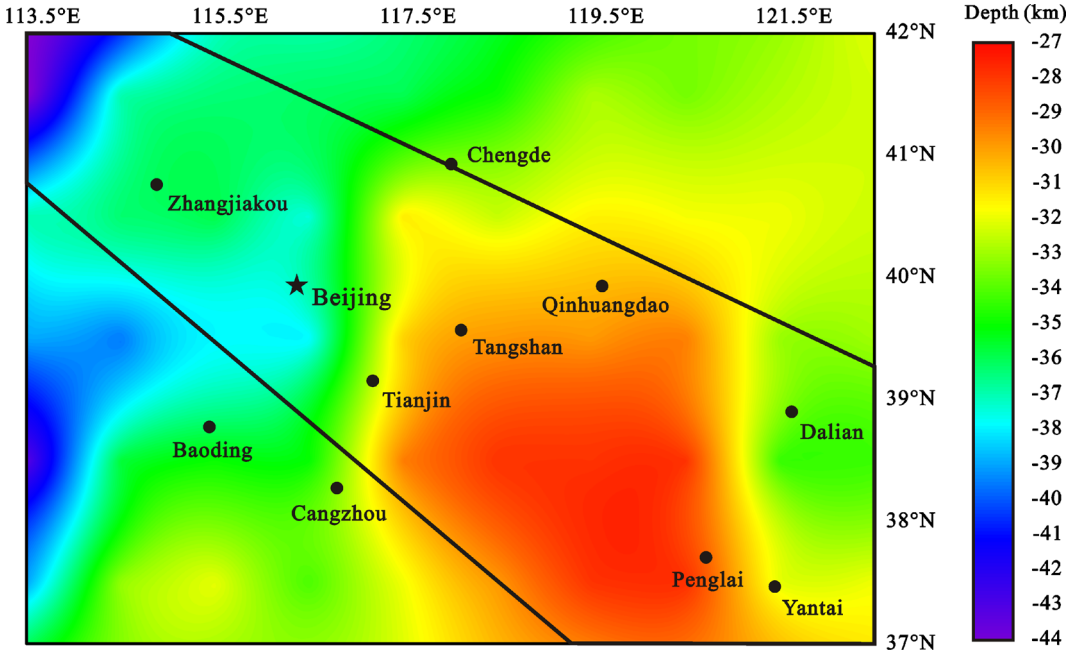

Figure 7. Depth map of the Moho surface beneath the BZSZ in North China. The western part of BZSZ has a deeper Moho surface, the maximum depth can reach about 44 km. The depth data are from CRUST 1.0 Model (Laske *et al.* 2013).

depth of the Mohr surface. Based on the modelling results and their relationship with the Moho surface depth, a deeper Moho surface generally favours stress accumulation in the upper layer and limits its accumulation in the lower layer. Therefore, in the BZSZ in North China, the upper layer of the Zhangjiakou area and the lower layer of the Penglai–Yantai area are more likely to experience earthquakes in the future.

Acknowledgements

We would like to express our deep gratitude to the two anonymous reviewers and the Associate Editor, Dr K Krishnamoorthy for their constructive comments and suggestions which improved this manuscript in many aspects. We wish to thank the China Earthquake Networks Center and the International Scientific and Technical Data Mirror Site, Computer Network Information Center, Chinese Academy of Sciences for earthquake data and topographic maps. This work was supported by the Fundamental Research Funds for the Central Universities (No. 2015QNA69) and the Priority Academic Program Development of Jiangsu Higher Educations Institutions.

References

Angelier J 2002 Inversion of earthquake focal mechanisms to obtain the seismotectonic stress IV – a new method free of choice among nodal planes; *Geophys. J. Int.* **150** 588–609.

Chen Y T, Huang L R, Lin B H, Liu M L and Wang X H 1979 A dislocation model of the Tangshan earthquake of 1976 from the inversion of geodetic data; *Acta Geophys. Sin.* **22(3)** 201–217 (in Chinese with English abstract).

Chen L W, Lu Y Z, Zhang J, Xu G L and Guo R M 1999 3D tectonic stress field in North China; *Acta Seismol. Sin.* **21(2)** 140–149 (in Chinese).

Chen L W, Lu Y Z, Guo R M, Xu G L and Zhang J 2001 Evolution of 3D tectonic stress field and fault movement in North China; *Acta Seismol. Sin.* **14(4)** 371–383.

Delvaux D and Barth A 2010 African stress pattern from formal inversion of focal mechanism data; *Tectonophys.* **482** 105–128.

Delvaux D and Sperner B 2003 Stress tensor inversion from fault kinematic indicators and focal mechanism data: The TENSOR program; In: New insights into structural interpretation and modeling (ed.) Nieuwland D, *Geol. Soc. London Spec. Publ.* **212** 75–100.

Fang Y and Zhang J 2009 Study of the segmentary activities in the Zhangjiakou–Bohai Fault System; *Earthquake* **29** 136–140 (in Chinese with English abstract).

Feng D Y, Liu X L, Su L D and Mei S Y 1996 Three-dimensional numerical simulation and analysis of seismogenic condition and temporo-spatial evolution of precursor field of Tangshan M=7.8 great earthquake; *North China Earthq. Sci.* **14(4)** 43–52 (in Chinese with English abstract).

Fischer K and Henk A 2013 3-D geomechanical modelling of a gas reservoir in the North German Basin: Workflow for model building and calibration; *Solid Earth Discuss.* **5** 767–788.

Fu Z X, Liu J and Liu G P 2004 On the long-term seismic hazard analysis in the Zhangjiakou–Penglai seismotectonic zone, China; *Tectonophys.* **390** 75–83.

Gao Z W 2001 A study on the characteristics of earthquake geology of the Zhangjiakou–Penglai Fault Zone; Dissertation, Institute of Geology, China Earthquake Administration (in Chinese with English abstract).

Gao W X and Ma J 1993 Seismo-Geological Background and Earthquake Hazard in Beijing Area; Geological Publishing House, Beijing (in Chinese).

Gao Z W, Xu J, Song C Q and Sun J B 2001 The segmental character of Zhangjiakou–Penglai Fault; *North China Earthq. Sci.* **19(1)** 35–42 (in Chinese with English abstract).

Han K 2009 Research on the segmentation and seismic activity characteristics of Zhangjiakou–Bohai Structural Zone; Dissertation, Institute of Geology, China Earthquake Administration (in Chinese with English abstract).

Hou G T, Ye L X and Du Q E 1999 Tectonic mechanism and geological significance of the Bo-Zhang Fault Zone; *Scientia Geol. Sin.* **34(3)** 375–380 (in Chinese with English abstract).

Hou G T, Wang Y X and Hari K R 2010 The Late Triassic and Late Jurassic stress fields and tectonic transmission of North China craton; *J. Geodyn.* **50** 318–324.

Hu M Q 2010 Study on contemporary tectonic deformation in North China by using three-dimensional simulation and parallel computation; Dissertation, Institute of Geology, China Earthquake Administration (in Chinese with English abstract).

Jaeger J C, Cook N G W and Zimmerman R W 2007 Fundamentals of rock mechanics; 4th edn, Blackwell Publishing, Oxford.

Jarosinski M, Beekman F, Matenco L and Cloetingh S 2011 Mechanics of basin inversion: Finite element modelling of the Pannonian Basin System; *Tectonophys.* **502** 121–145.

Ju W, Hou G T and Hari K R 2013a Mechanics of mafic dyke swarms in the Deccan Large Igneous Province: Palaeostress field modeling; *J. Geodyn.* **66** 79–91.

Ju W, Hou G T, Huang S Y and Ren K X 2013b Structural fracture distribution and prediction of the Lower Jurassic Ahe Formation sandstone in the Yinan–Tuzi area, Kuqa Depression; *Geotect. Metall.* **37** 592–602 (in Chinese with English abstract).

Ju W, Hou G T and Zhang B 2014 Insights into the damage zones in fault-bend folds from geomechanical models and field data; *Tectonophys.* **610** 182–194.

Ju W, Sun W F and Hou G T 2015 Insights into the tectonic fractures in the Yanchang Formation interbedded sandstone-mudstone of the Ordos Basin based on core data and geomechanical models; *Acta Geol. Sin-Engl.* **89(6)** 1986–1997.

Lai X L, Sun Y and Liu Z 2006 Study of deep seismic sounding in strongly seismic regions of North China; *J. Geod. Geodyn.* **26(1)** 55–62 (in Chinese with English abstract).

Laske G, Masters G, Ma Z T and Pasyanos M 2013 Update on CRUST 1.0 – a 1-degree global model for earth's crust; *Geophys. Res. Abstr.* **15** EGU2013-2658.

Li T Z and Wang G D 1981 A preliminary analysis of the earthquake-controlling and the earthquake-generating tectonics; *J. Seismol. Res.* **4(3)** 312–317 (in Chinese with English abstract).

Li J H, Hao S J and Hu Y T 1999 New evidence and analyses for the NWW trending Changping–Fengnan Fault; *Seism. Geol.* **21(2)** 176–184 (in Chinese with English abstract).

Li Y X, Xu J, Chen J Z, Zhang J H and Zhang Z F 2006 Basic characteristics of current strain field in the epicentral area of Xingtai, Bohai, Haicheng and Tangshan strong earthquake; *North China Earthq. Sci.* **24(2)** 36–39 (in Chinese with English abstract).

Li X S, Liu B H, Hua Q F, Zhao Y X and Liu C G 2009 Characters of the Zhangjiakou–Penglai Fault Zone activity in the Bohai Sea since Late Quaternary; *Adv. Marine Sci.* **27(3)** 332–341 (in Chinese with English abstract).

Liu F T, Qu K X, Wu H, Li Q, Liu J H and Hu G 1986 Seismic tomography of North China region; *Acta Geophys. Sin.* **29(5)** 442–449 (in Chinese with English abstract).

Liu Q Y, Wang J, Chen J H, Li S C and Guo B 2007 Seismogenic tectonic environment of 1976 great Tangshan Earthquake: Results from dense seismic array observations; *Earth Sci. Front.* **14(6)** 205–213.

Liu C, Shi Y L, Zheng L and Zhu B J 2012 Relation between earthquake spatial distribution and tectonic stress accumulation in the North China Basin based on 3D viscoelastic modeling; *Acta Geophys. Sin.* **55(12)** 3942–3957 (in Chinese with English abstract).

Lunina O V and Gladkov A S 2007 Late Cenozoic fault pattern and stress fields in Barguzin rift (Baikal region); *Russ. Geol. Geophys.* **48** 598–609.

Martinez-Martinez J, Benavente D and Garcia-del-Cura M A 2012 Comparison of the static and dynamic elastic modulus in carbonate rocks; *B. Eng. Geol. Environ.* **71** 263–268.

Mei S R and Liang B Y 1989 A mathematical simulation for seismogenetic process of the Tangshan earthquake; *Earthq. Res. China* **5** 9–17 (in Chinese with English abstract).

Mockovciakova A and Pandula B 2003 Study of the relation between the static and dynamic moduli of rocks; *Metalurgija* **42** 37–39.

Rao M V M S, Prasanna Lakshmi K J, Sarma L P and Chary K B 2006 Elastic properties of granulite facies rocks of Mahabalipuram, Tamil Nadu, India; *J. Earth Syst. Sci.* **115** 673–683.

Shi Y L and Cao J L 2008 Effective viscosity of China continental lithosphere; *Earth Sci. Front.* **15** 83–95 (in Chinese with English abstract).

Smart K J, Ferrill D A and Morris A P 2009 Impact of interlayer slip on fracture prediction from geomechanical models of fault-related folds; *AAPG Bull.* **93** 1447–1458.

Song H G, Gao W A, Sun J X and Jiang W 1982 Numerical analysis of stress field of Tangshan area applying three dimensional finite element method to compute focal stress field; *Northwestern Seismol. J.* **4** 49–56 (in Chinese with English abstract).

Sperner B, Muller B, Heidbach O, Delvaux D, Reinecker J and Fuchs K 2003 Tectonic stress in the Earth's crust: Advances in the World Stress Map Project; In: New insights into structural interpretation and modeling (ed.) Nieuwland D, *Geol. Soc. London Spec. Publ.* **212** 101–116.

Suo Y H, Li S Z, Liu X, Dai L M, Xu L Q, Wang P C, Zhao S J and Zhang B K 2013 Structural characteristics of NWW-trending active fault zones in east China: A case study of the Zhangjiakou–Penglai Fault Zone; *Acta Petrol. Sin.* **29** 953–966 (in Chinese with English abstract).

Wang M G and Li C C 2005 The mian fault in Hebei Plian and its distribution and activity character; *J. Hebei. Inst. Technol.* **27** 113–118 (in Chinese with English abstract).

Wang F Y, Zhang X K, Chen Y, Li L, Chen Q F, Zhao J R, Zhang J S and Liu B F 2004 2-D P-wave velocity structure in the mideast segment of Zhangjiakou–Bohai tectonic zone: Anxin–Xianghe–Kuancheng DSS profile; *Acta Seismol. Sin.* **17** 32–42.

Wang R B, Gu G H, Xu J and Zhou W 2005 Discussion on characteristics of crustal deformation along the Zhangjiakou–Bohai Sea Seismotectonic Zone; *Earthq. Res. China* **19** 327–337.

Wu F Y, Lin J Q, Wilde S A, Zhang X O and Yang J H 2005 Nature and significance of the Early Cretaceous giant igneous event in eastern China; *Earth Planet Sci. Lett.* **233** 103–119.

Xiang H F, Fang Z J, Xu J, Li R C, Jia S F, Hao S J, Wang J B and Zhang W X 1988 Research on the tectonic settings and strong earthquakes' repetition in Sanhe–Pinggu (M=8) earthquake region; *Seismol. Geol.* **101** 15–28 (in Chinese).

Xie F R, Cui X F, Zhao J T, Chen Q C and Li H 2004 Regional division of the recent tectonic stress field in China and adjacent areas; *Chinese J. Geophys.* **47** 654–662 (in Chinese with English abstract).

Xu J, Song C Q and Chu Q Z 1998 Preliminary study on the seismotectonic characters of the Zhangjiakou–Penglai Fault Zone; *Seismol. Geol.* **20** 146–154 (in Chinese with English abstract).

Xu X W, Wu W M, Zhang X K, Ma S L, Ma W T, Yu G H, Gu M L and Jiang W L 2002 The latest crustal tectonic deformation and earthquakes in the Capital Circel Region of China; Science Press, Beijing (in Chinese).

Xue Z Z 1986 The relationship between focal depth and crustal structure for Tangshan earthquake; *Seismol. Geol.* **8** 69–78 (in Chinese with English abstract).

Yang G H, Han Y P and Zhou X Y 2002 New features of crustal motion in North China; *J. Geod. Geodyn.* **22** 28–33 (in Chinese with English abstract).

Yao C Y, Zhou R L, Hu A G and Li Y L 2012 Determination of Young's modulus by using conventional logging: Take upper Paleozoic reservoirs of Fuxian block as example; *Petrol. Geol. Eng.* **26** 110–112 (in Chinese with English abstract).

Yin A 1991 Mechanisms for the formation of domal and basinal detachment faults: A three-dimensional analysis; *J. Geophys. Res.* **96(B9)** 14577–14594.

Yuan J R, Xu J S and Gao S J 1999 Back analysis of present tectonic stress field in North China region using GPS data; *Acta Geosci. Sin.* **20** 232–238 (in Chinese with English abstract).

Zang S X, Li C, Ning J Y and Wei R Q 2003 A preliminary model for 3-D rheological structure of the lithosphere in the North China; *Science China Ser. D-Earth Sci.* **46** 461–473.

Zeng W T, Ding W L, Zhang J C, Zhang Y Q, Guo L, Jiu K and Li Y F 2013 Fracture development in Paleozoic shale of Chongqing area (South China). Part two: Numerical simulation of tectonic stress field and prediction of fractures distribution; *J. Asian Earth Sci.* **75** 267–279.

Zhan Z M, Chen L W and Lu Y Z 2011 Crustal dynamic parameters and 3D finite element model of North China; *J. Geod. Geodyn.* **31** 28–32 (in Chinese with English abstract).

Zhang C K, Zhang X K, Zhao J R, Ren Q F, Zhang J S and Hai Y 2002 Study and review on crust-mantle velocity structure in Bohai Bay and its vicinity; *Acta Seismol. Sin.* **15** 447–455.

Zhao G Z, Liu T S, Jiang Z, Tang J, Xu C F, Zhan Y, Bai D H and Liu G D 1997 Investigation on MT data along Yanggao-Rongcheng profile by two-dimensional inversion;

Acta Geophys. Sin. **40** 38–46 (in Chinese with English abstract).

Zhu R X, Chen L, Wu F Y and Liu J L 2011 Timing, scale and mechanism of the destruction of the North China Craton; *Science China Ser. D-Earth Sci.* **54** 789–797.

Zhu R X, Yang J H and Wu F Y 2012 Timing of destruction of the North China Craton; *Lithos* **149** 51–60.

Zoback M L 1992 First- and second-order patterns of stress in the lithosphere: the world stress map project; *J. Geophys. Res.* **97** 11703–11728.

MS received 2 December 2015; revised 26 February 2016; accepted 23 March 2016

Corresponding editor: K Krishnamoorthy